Band-gap variation in Mg- and Cd-doped ZnO nanostructures and molecular clusters

Manoj K. Yadav, Manoranjan Ghosh, Ranjit Biswas, Arup K. Raychaudhuri, and Abhijit Mookerjee
Unit for Nanoscience and Technology, S.N. Bose National Center for Basic Sciences, JD Block, Sector III, Salt Lake City, Kolkata 700 098, India

Soumendu Datta
Department of Materials Science, S.N. Bose National Center for Basic Sciences, JD Block, Sector III, Salt Lake City, Kolkata 700 098, India

(Received 19 April 2007; revised manuscript received 12 September 2007; published 30 November 2007)

We study the effect of doping on band gap in Mg- and Cd-doped zinc oxide nanostructures and molecular clusters. The fabrication of doped nanostructures was carried out via solution route. The lower doping efficiency of Cd than that of Mg has been explained in terms of binding energy. The band gap varied from 3.04 eV in Cd-doped (9.1 at. % of Cd) nanostructure to 3.99 eV in Mg-doped (16.8 at. % of Mg) nanostructure. Theoretical analysis using first-principles molecular dynamics techniques on pristine and doped ZnO clusters shows that the energy gap between the highest occupied molecular orbital and the lowest unoccupied molecular orbital exhibits a similar variation as does the band gap in nanostructures with the varying concentration of Mg and Cd.

DOI: 10.1103/PhysRevB.76.195450 PACS number(s): 61.46.Df, 36.40.−c, 71.15.Nc

I. INTRODUCTION

ZnO and doped ZnO are important in technological applications in catalytic, electrical, optoelectronic,[1,2] and quantum devices.[3,4] ZnO is a direct-band-gap semiconductor with a large gap of 3.37 eV. A large variety of ZnO nanostructures such as nanoparticles, nanorods, nanotubes, and nanowires have been synthesized[5,6] and they have been successfully used in, for example, optical devices.[7,8] For the realization of devices based on ZnO, one of the prerequisites is to engineer the size of the band gap. One of the ways of doing this is to alloy ZnO with specific concentrations of materials such as MgO and CdO.

To this end, there have been several theoretical[9,10] and experimental[12–15] works. Ohtomo *et al.*[12] alloyed ZnO with MgO using the pulsed laser deposition (PLD) method and reported increase in band gap in the alloy. A decrease in band gap in Cd-doped ZnO has been reported by several authors.[14–16] Makino *et al.*[15] have studied alloying of ZnO with CdO using PLD method and found a decrease in the band gap in the alloy. Wang *et al.*[14] investigated the effect of Cd substitution in $Zn_{(1-x)}Cd_xO$ nanorods and nanoneedles. They also found a decrease in the band gap with increasing concentration of Cd. Kukreja *et al.*[16] could have achieved a band gap of about 3.8 eV by alloying ZnO with MgO. In the case of alloying ZnO with CdO, they were able to attain a band gap as low as 2.9 eV.

To understand the behavior of these materials, it is imperative to study both their crystal and electronic structures. There have been a few completely first-principles attempts to look at the electronic structure of ZnO from a density-functional viewpoint.[18–22] Most interesting phenomena occur at the surface of these compound semiconductors. It is certainly true that there are some properties of these compounds that are *local*, in the sense that they occur at a specific location of the surface, for example, adsorption or surface catalysis. It may therefore be useful to study clusters of these compounds whose electronic and structural properties will give insight into these local properties.[23,24]

As clusters bridge the gap between a molecule and the bulk material, in this work we have tried to understand, at least qualitatively, our experimental findings on $Zn_{(1-x)} \times (Mg,Cd)_xO$ nanostructures (10–15 nm) through a first-principles theoretical study of clusters of sizes about 6 Å. Though it is perhaps not fair to compare two systems which differ in size by an order of magnitude, the aim of this investigation is to look at qualitative trends with increasing doping.

Here, we have carried out a systematic first-principles theoretical study of clusters of $(ZnO)_n$ using the soft-pseudopotential technique ideally set up for clusters containing an element with *d* electrons whose potentials are sufficiently localized and deep. Such a formulation is ideal for Zn containing clusters. We shall determine the ground state shapes of the clusters as well as that of the next higher energy isomer in the size range $1 \leq n \leq 12$. We shall also examine some of the energetics of the clusters as a function of their cluster size. It would also be interesting to study the variation of the band gap with varying doping concentrations in nanosized samples from first principles. The smallest cluster size in the range of a few nanometers in diameter would involve around 48–50 ZnO units. Before we carry out a full-fledged first-principles molecular dynamical analysis of such large clusters, we shall first study some of the smaller stable or magic clusters of ZnO, whose structural and electronic properties were studied earlier.[11] We shall dope them with Mg and Cd and study the variation of the bonding energy and the highest occupied molecular orbital-lowest unoccupied molecular orbital (HOMO-LUMO) gap which is the "band gap" in these finite systems. An overwhelming majority of such studies to date follow techniques which are based on the density-functional theory in the local density approximation (LDA). The band gap which arises out of the Kohn-Sham *virtual* orbital based density of states in the LDA is always underestimated. We shall therefore concentrate on the *change* in the band gap (or the HOMO-LUMO gap) on doping, with the expectation that the errors in the doped and undoped cases compensate each other.

We have then doped some of the stable pristine $(ZnO)_n$ clusters with Mg and Cd and have shown that the HOMO-LUMO gaps in the smaller doped clusters show similar increase or decrease with doping concentration as do the band gaps in larger ZnO nanostructures. We have also shown that this qualitative similarity becomes more pronounced as we increase the size of the clusters.

We shall use our theoretical analysis to examine the experimental study of $Zn_{(1-x)}(Mg,Cd)_xO$ alloy nanostructures synthesized in our laboratory using the acetate route. We should note that majority of the experimental works have been carried out on epitaxially grown films on substrates. Our emphasis in this work is on nanostructures of ZnO and Cd- and Mg-doped ZnO. While there are several experimental reports elaborating the variation of band gap in doped ZnO, very few works can be found in this direction, certainly for nanostructures of average size ~100 Å.[25] This is because the synthesis and characterization of molecular clusters of the order of 10 Å are difficult.

For the synthesis of $Zn_{(1-x)}(Mg,Cd)_xO$ alloy nanostructures, we have chosen a solution growth method for clear understanding of lower doping efficiency of Cd than that of Mg. In this method, mixing occurs at an atomic level. Consequently, the material so made is close to thermodynamic equilibrium. Therefore, the doping efficiency of Mg and Cd into ZnO can be explained on the basis of cohesive binding energy of the corresponding alloys. The change in the binding energies of $Zn_{(1-x)}Mg_xO$ and $Zn_{(1-x)}Cd_xO$ alloy molecules from the parent compound ZnO determines the doping efficiency of corresponding dopant atoms.

One needs to be cautious while investigating the effect of doping on the band gap of ZnO nanostructures because in the quantum confinement regime, band gap becomes a function of size.[26] In our experimental work, we have used nanostructures of size 10–15 nm, which lies beyond the quantum confinement limit (≤5 nm). In the size regime we are working (10–15 nm), the variation in the band gap for small fluctuations in size (~5 nm) is very small (0.06 eV) compared to the change in band gap observed as the effect of doping.

We should note that any LDA calculation will underestimate the band gap. In particular, the band gap of bulk ZnO which is around 3.3 eV is grossly underestimated in all such calculations. However, the change in the band gap will be more reliable, assuming cancellation of errors. There have been experiments on the band-gap change in thin films of ZnO.[15,27] The changes (18% enhancement with 33% Mg doping and 10% decrease with 7% Cd doping) found by both works are roughly consistent with the nanoparticle results quoted here. Experimental works are lacking on bulk $Zn_{1-x}Mg_xO$ and $Zn_{1-x}Cd_xO$ alloys. The LDA theoretical work by Thangavel *et al.*[9] on these bulk alloys indicate much larger changes in the bulk alloys: 158% enhancement with 50% concentration of Mg and 85% enhancement with 50% concentration of Cd. Our calculations by both VASP and TB-LMTO also show very similar large changes in the bulk alloys. It would be interesting to understand why the clusters and thin films behave similarly and the bulk changes are so much larger.

II. EXPERIMENTAL DETAILS

The details of experiments on the Mg- and Cd-doped ZnO nanostructures have been reported earlier by some of us in two earlier papers.[25,28] In this section, we shall give a gist of the preparational and characterization techniques used and a summary of the results relevant to this paper.

A. Synthesis

ZnO nanostructures were synthesized using acetate route. A 0.03*M* NaOH solution in ethanol was added in 0.01*M* solution of $Zn(CH_3COOH)_2,2H_2O$ in ethanol kept at 65 °C. The final solution was stirred and heated at 65 °C for 2 h. This method allows precipitation of ZnO nanoparticles and avoids precipitation of hydroxides if the temperature is above 60 °C. For the purpose of making $Zn_{1-x}Mg_xO$ alloys, we added different amounts of $Mg(CH_3COOH)_2,4H_2O$ to the $Zn(CH_3COOH)_2,2H_2O$ solution for different doping concentrations. The dispersions containing $Zn_{1-x}Mg_xO$ nanoparticles were washed with water by centrifugation. Finally, the precipitates were collected by dispersing them in ethanol for optical measurements.

The fabrication of $Zn_{1-x}Cd_xO$ nanostructures was not possible under similar conditions as described above. This is because of the fact that incorporation of Cd into ZnO leads to the decrease in cohesive binding energy (see Fig. 9). To achieve proper alloying, the $Zn_{1-x}Cd_xO$ nanostructures were synthesized under high pressure (54 atm) to obtain higher boiling point of ethanol (230 °C). In order to synthesize $Zn_{1-x}Cd_xO$ alloy nanostructures, a clear solution of 0.015*M* $Zn(CH_3COOH)_2,2H_2O$, 0.045*M* NaOH, and controlled amount of $Cd(CH_3COOH)_2,2H_2O$ was prepared. Then, the solution was taken in Teflon lined autoclaves preset at 230 °C. The $Zn_{1-x}Cd_xO$ nanostructures thus prepared after 2 h reaction within the autoclaves were centrifuged and washed by water. The precipitates were collected by dispersing in ethanol for optical measurements.

B. Characterization

The amounts of incorporated dopant atoms in the alloy nanostructures were found by inductively coupled plasma atomic emission spectroscopy. The maximum incorporation achieved in $Zn_{1-x}Mg_xO$ and in $Zn_{1-x}Cd_xO$ were $x=0.17$ and 0.091 for the two alloys, respectively. Incorporation beyond these values could not be achieved as the phase segregation starts to take place. The average size of the nanostructures was determined by transmission electron microscope (TEM) as well as x-ray diffractometer (XRD) data. The average size of undoped ZnO nanostructures lies in the range 10–15 nm as seen by TEM image shown in the left panel of Fig. 1. The size of the alloy nanostructures was also found to lie in the same range. Two representative TEM images of $Zn_{1-x}Cd_xO$ and $Zn_{1-x}Mg_xO$ alloy nanostructures are shown, respectively, in the middle and right panels of Fig. 1. The sizes of the nanostructures were also determined by Williamson-Hall analysis[29] of the XRD data and the results agree well with the TEM results.

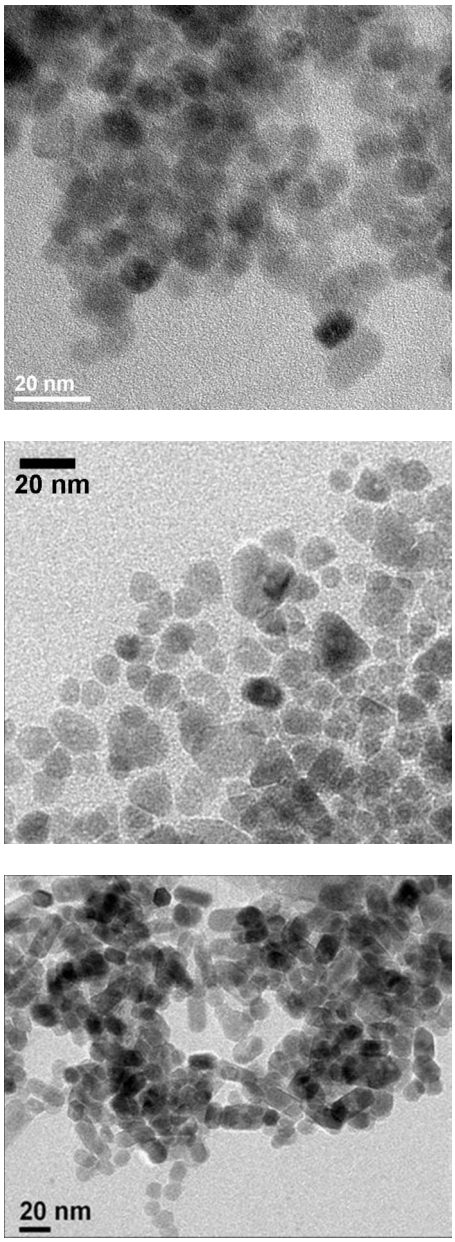

FIG. 1. TEM images of (left) undoped ZnO nanostructures, (middle) Cd-doped ZnO nanostructures, and (right) Mg-doped nanostructures.

C. Results and discussion

The direct-band-gap values of ZnO and its alloy nanostructures have been determined by monitoring the fundamental absorption edges of the room temperature absorption spectra shown in Fig. 2. In the left panel of that figure, we can see the gradual blueshift of the fundamental absorption edge with the increase of Mg concentration. Also, the excitonic peak appearing in the absorption spectra of ZnO persists even after considerable increase in Mg incorporation. The band gap of $Zn_{1-x}Mg_xO$ nanostructures increases monotonously as we increase the Mg concentration. At 16.8% Mg concentration, we could achieve a band gap of 3.99 eV, which is equivalent to 12.39% enhancement. On the other hand, Cd-doped nanostructures show a gradual redshift in fundamental absorption edge, as shown in the right panel of Fig. 2. We could achieve a band gap as low as 3.04 eV at 9.10% Cd concentration. Kukreja *et al.*[16] have reported 12.76% enhancement in the band gap in Mg-doped ZnO alloy at 14% Mg concentration. In the case of Cd-doped ZnO alloy, they have found about 13.95% decrease in the band gap at 8.0% Cd concentration. In both cases, our results compare well even though the methods of fabrications were quite different. We have fabricated nanostructures via solution route, whereas Kukreja *et al.*[16] have made alloy by the PLD method. Interestingly, for the $Zn_{1-x}Cd_xO$ alloy nanostructures, the excitonic behavior of the absorption spectra diminishes quickly as soon as Cd incorporation starts to take place. Thus, the large excitonic binding energy of ZnO (60 meV) decreases sharply for $Zn_{1-x}Cd_xO$, contrary to the case of $Zn_{1-x}Mg_xO$.

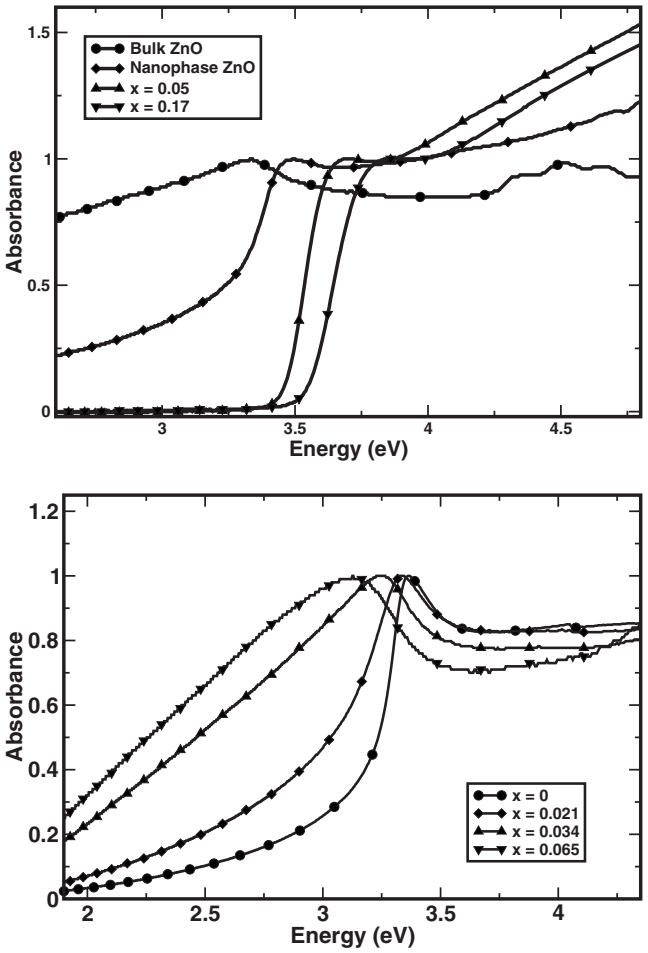

FIG. 2. Absorption spectra of the nanostructures: (left) Mg-doped nanostructure and (right) Cd-doped nanostructure.

III. THEORETICAL METHODOLOGY

The basis of our electronic and total energy calculations and shape optimization of the clusters will be the projector augmented wave (PAW) method. Blöchl[30] combined the density-functional based multiple scattering (the linearized

augmented plane wave) and the pseudopotential approaches to present the computationally elegant, transferable, and accurate PAW. Kressé and Joubert[31] modified and coded this PAW technique into the Vienna *ab initio* pseudopotential package (VASP) on which our present work will be based.

The mathematics of the PAW method has been described in detail elsewhere.[30] We shall comment on the following.

(1) The electron-ion interaction was described by the pseudopotential based ideas. This is implicit in the PAW methodology.

(2) We have used the exchange-correlation functional suggested by Perdew *et al.*[32]

(3) The clusters were placed in cells surrounded by vacuum and periodic boundary conditions were used. The size of the supercell was large enough (cube of 15 Å) to avoid interaction between the images. Typically, in the case of $(ZnO)_{12}$, the distance between its two images was greater than 9 Å.

(4) Gamma point calculations[33] have been performed with the plane wave cutoff energy of 525 eV.

(5) The geometries of the clusters have been optimized using conjugate gradient algorithm and the convergence was achieved until the maximum force on each ion was less than 0.01 eV/Å.

The binding energies of $(ZnO)_n$ clusters are defined as follows:

$$E_B = E(n) - n[E(\mathrm{Zn}) + E(\mathrm{O})], \quad (1)$$

where $E(n)$ is the total energy of the $(ZnO)_n$ cluster, $E(\mathrm{Zn})$ is the energy of a single Zn atom, and $E(\mathrm{O})$ is the energy of a single O atom. As for MgO clusters in earlier works,[34] we have fitted the binding energies, per ZnO unit, of the clusters $(2 \leqslant n \leqslant 12)$ in order to get the value of the energy for larger clusters by extrapolation. The fitted expression is given by

$$E_B/n = -24.33n^{-1} + 45.12n^{-2/3} - 22.53n^{-1/3} - 3.78. \quad (2)$$

This functional form is valid only for small values of n and fits our data for $n=2,\ldots,12$. We have calculated the cohesive energy per ZnO unit for bulk ZnO and it comes out to be 7.26 eV as against the experimental value of 7.52 eV.

The second difference in binding energy may be calculated as

$$\Delta_2 E(n) = 2E(n) - E(n+1) - E(n-1), \quad (3)$$

where $E(n+1)$ and $E(n-1)$ are energies of $(ZnO)_{n+1}$ and $(ZnO)_{n-1}$ clusters, respectively. The quantity $\Delta_2 E(n)$ represents the relative stability of a cluster of size n with respect to its neighbors. This quantity may be compared with mass spectrographs of a substance.

The energy gap E_g between the HOMO and the LUMO for the ground state structure of each cluster is the HOMO-LUMO gap. The stability of a particular structure can be predicted with the magnitude of E_g. The structure having a larger gap is more stable and vice versa.

A. Pristine ZnO clusters

We shall begin with a brief description of the ground state and next higher energy local minimum state structures of $(ZnO)_n$ clusters before we describe overall trends with size.

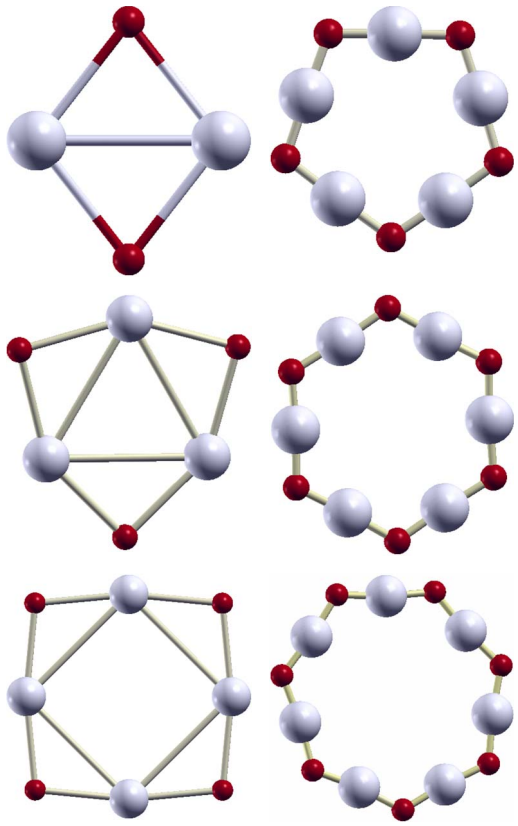

FIG. 3. (Color online) Ground state structures of $(ZnO)_n$ clusters for $n=2-7$; large light spheres represent Zn atoms and smaller darker spheres the O atoms. [Figures drawn using Xcrysden (Ref. 17).]

The structures of the ground states of $(ZnO)_n$ clusters for $n=2-7$ are shown in Fig. 3. All the structures are planar, distorted polygons with D_{nh} symmetries. The Zn-O-Zn angles begin with 75° at $n=2$ and monotonically increase to 122° for $n=7$, while the O-Zn-O angles begin with 105° for $n=2$ and become almost 180° for $n=6$ and $n=7$.

We have observed that there is a competition between planar and three-dimensional structures. For $n \leqslant 7$, ringlike planar structures are more stable. At a critical size of $n=8$, there is a transition of stability from planar rings to three-dimensional ground state structures. By the time we reach $(ZnO)_7$, the difference in energy between the planar and the three-dimensional nearest isomers structures is already less than 50 kJ/mol. For $(ZnO)_8$, the ground state structure which is two $(ZnO)_4$ rings attached atop each other with $(ZnO)_2$ units belongs to D_{4d} symmetry. It is at this size that formation of spheroidal structures reminiscent of fullerenes reported by Behrman *et al.*[35] begins to show up. Now, as the three-dimensional structures stabilize, the average Zn-O bond length suddenly increases dramatically.

Figure 4 shows the ground state and next higher energy structures for $(ZnO)_n$, $n=8,\ldots,12$. Now, the structures are built out of $(ZnO)_3$ and $(ZnO)_2$ units, i.e., hexagons and squares. This tendency of forming spheroidal structures with these units is characteristic of ZnO clusters with large n. The $(ZnO)_{12}$ is the most spheroidal in shape in the size range 2

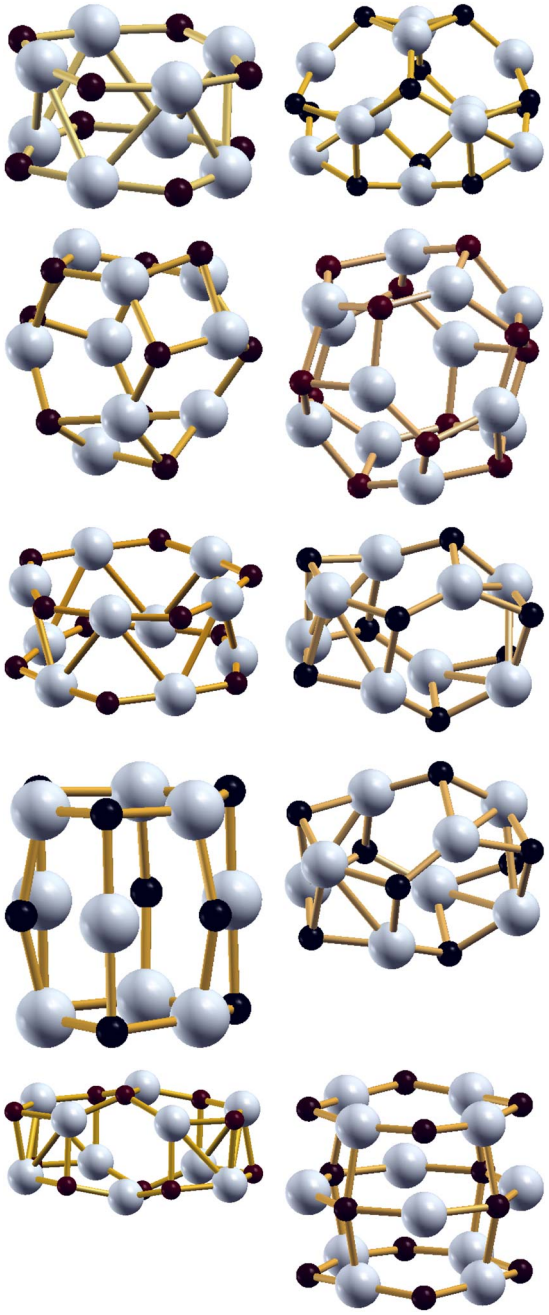

FIG. 4. (Color online) $(ZnO)_n$ clusters for $n=8-12$; large light (gray) spheres represent Zn atoms and smaller dark (red) spheres the O atoms. The subscripts g and l stand for global and local minima structures, respectively.

$\leqslant n \leqslant 12$. In this, it resembles C_{60}, but unlike it, it is unstable with respect to the macroscopic crystal. These structures differ from the fullerenes in the sense that while fullerenes have pentagons and hexagons, these structures have squares and hexagons. Here, we do not expect pentagons, since that will force like atoms to bond, which is energetically unfavorable in the case of ZnO. This tendency of forming spheroidal structures appears to be rather surprising. We would have expected compact shapes as found by Behrman *et al.*[35] for NaCl. As the size increases, the Zn-O distance decreases toward the bulk value.

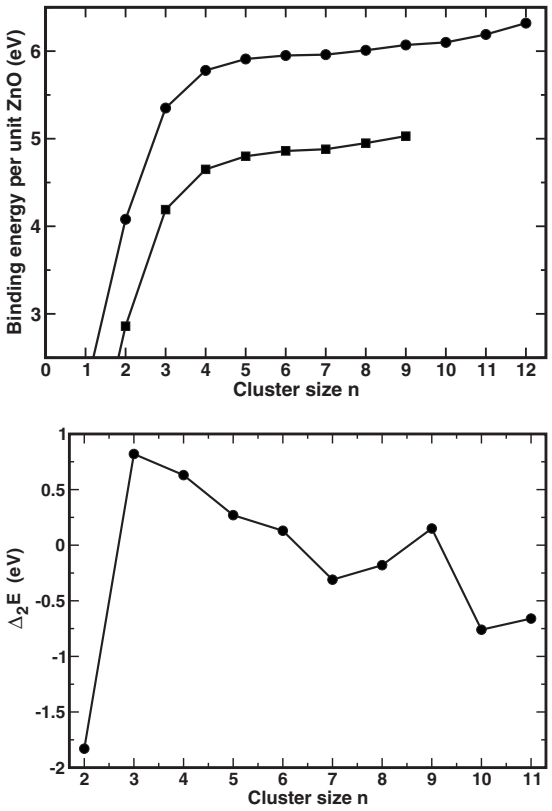

FIG. 5. (Top) Binding energy per ZnO unit versus size of cluster n. The circles are results of this work, while the squares are from Ref. 23. (Bottom) Second difference in binding energy versus size of cluster n.

The higher energy isomers for $n=8,\ldots,12$ are also shown in Fig. 4. These are more open towerlike structures reminiscent of MgO ground states found by Calvo.[34] For ZnO, these are not stable shapes.

We next examine the energetics of the clusters. Figure 5 (top) shows the binding energy in $(ZnO)_n$ clusters per ZnO units. The points indicate the calculated energies in eV and the line shows the fitted form mentioned earlier in Eq. (2). The form is empirical and has been suggested by many authors.[23] It seems to fit the binding energy quite well over the entire range of cluster sizes. Our calculations, however, throw no light upon its exact form. However, the binding energy per ZnO unit in bulk ZnO is around 7.52 eV.[36] The binding energy curve tends toward this value slowly and we are nowhere near approaching this limit for clusters as small as 12 units.

Our results match those of an earlier work by Matxain *et al.*[23] qualitatively. There is a rigid shift when we compare the two. Matxain *et al.* also used a density-functional based method; however, the pseudopotentials used in the two works are quite different. We have used the latest projector wave formalism eminently suitable for atoms with deep d levels as in Zn. The binding energies of Matxain *et al.* were consistently lower than ours, almost by a rigid shift across the cluster size domain. Using the same PAW technique, we have calculated the cohesive energy per ZnO unit for the bulk. The work of Matxain *et al.* does not quote the bulk

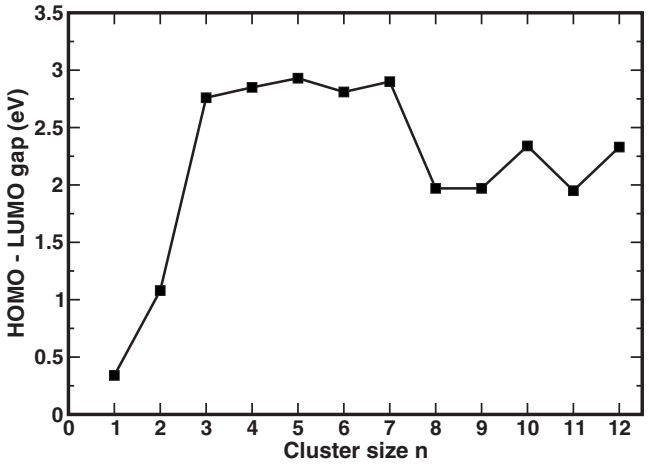

FIG. 6. HOMO-LUMO gap versus size of pristine ZnO clusters of n units.

value and the fitted curve to their calculations for small clusters is valid only for small values of n and cannot be extrapolated for large n. However, a comparison between our two curves indicates a rigid shift between them, which should be the difference in the cohesive energy per ZnO unit of the bulk in the two cases.

The second difference in binding energies $\Delta_2 E$ is shown in Fig. 5 (bottom). This indicates the relative stability of the clusters with respect to its neighboring sizes. This is consistent with our other inferences from bond lengths and cluster shapes and may be compared with the mass spectrograph of ZnO clusters. These stable clusters then neither add another unit and stabilize themselves nor shed a unit to do so, and these sizes show peaks in the mass spectrograph. Bulgakov *et al.*[37] have carried out laser ablation synthesis of ZnO clusters and have shown from a time of flight mass spectra the stability of clusters of sizes $n=6$, 9, and 11. Their proposed shapes for the $n=9$ and $n=11$ clusters closely agree with our prediction.

Figure 6 shows the HOMO-LUMO gaps as a function of cluster size. As expected, large gaps in the planar ring structures indicate their stability. There is a transition at $n=8$, as expected, a signature of the planar to three-dimensional structures. Of these, the $n=9$ cluster appears most stable, as indicated by $\Delta_2 E$.

B. Doped ZnO clusters

We have chosen a 12-molecule ZnO cluster as it is relatively more stable than others in the small cluster range.[38] The undoped $(ZnO)_{12}$ cluster is almost spherical in shape and resembles almost fullerene structure. The exact fullerene structure, however, consists of hexagonal and pentagonal units, whereas this $(ZnO)_{12}$ structure consists of units of rhombus and hexagons. The total cohesive binding energy of $(ZnO)_{12}$ cluster is 75.89 eV and its HOMO-LUMO gap is 2.33 eV.

We have carried out substitutional doping of $(ZnO)_{12}$ cluster, that is, replacing Zn atom(s) by dopant atom(s). We have tried to place the dopant atoms as random as possible to avoid impractical segregated structure. Figure 7 shows the structures of doped $(Zn_{12-n}Mg_n)O_{12}$ clusters doped with up to five Mg atoms. The largest Zn–O bond length in an undoped $Zn_{12}O_{12}$ cluster is 1.97 Å. The inclusion of Mg atoms reduces the average bond length as Mg-O bond lengths vary only between 1.90 and 1.94 Å. This observation suggests greater stability to the Mg-doped cluster compared to an undoped ZnO cluster. The structures of $(Zn_{12-n}Cd_n)O_{12}$ clusters doped with up to five Cd atoms are shown in Fig. 8. The Cd-O bond lengths in these clusters vary between 2.10 and 2.18 Å, thus making the clusters relatively less stable.

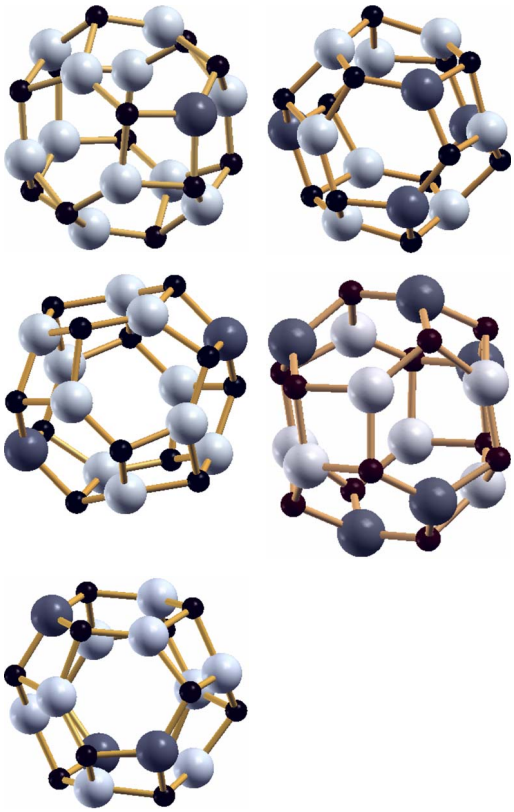

FIG. 7. (Color online) Structures of Mg-doped $(ZnO)_{12}$ clusters; lightly shaded large spheres represent Mg atoms, white large spheres represent Zn atoms, and smaller black spheres represent O atoms.

C. Result and discussion

The left panel in Fig. 9 shows the variation of binding energy of the clusters with increasing concentration of dopant atoms. The total binding energy of these doped clusters increases with increasing concentration of Mg, whereas it decreases with increasing Cd concentration. This means that doping with Mg increases the stability of the clusters, whereas doping with Cd decreases stability. This is an important observation that connects with the following experimental facts: (i) low doping efficiency of Cd compared to Mg and (ii) increase in photoluminescence peak of $Zn_{(1-x)}Cd_xO$. The lower stability of $Zn_{(1-x)}Cd_xO$ clusters gives rise to fluctuations in the Cd content of the material as

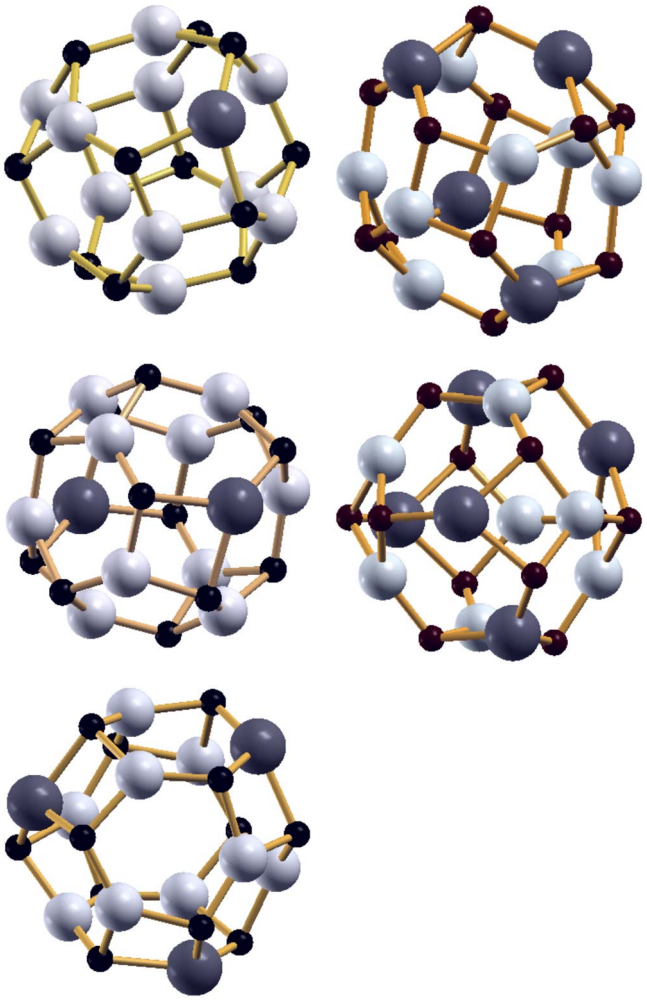

FIG. 8. (Color online) Structures of Cd-doped $(ZnO)_{12}$ cluster, lightly shaded spheres represent Zn atoms, small dark spheres represent O, and large dark spheres represent Cd.

well as overall lower Cd incorporation into ZnO as observed by several authors.[15,39]

The change in band gap with doping as we increase the size of the clusters is shown in the middle panel of Fig. 9. We notice that as the size increases, the change in the band gap approaches the experimental data. Our choice of the $(ZnO)_{12}$ cluster to analyze the experimental results appears to be justified.

The experimental variation in band gap in nanostructure and theoretically obtained HOMO-LUMO gap in $(ZnO)_{12}$ clusters with increasing concentration of Mg and Cd are compared in the right panel in Fig. 9. The value corresponding to zero percentage of dopant atom refers to the value of undoped ZnO structure. The HOMO-LUMO gap increases with increasing concentration of Mg and decreases with increasing concentration of Cd. A cluster with a larger HOMO-LUMO gap is more stable and vice versa. Therefore, the fact that the increase in Mg concentration increases the HOMO-LUMO gap and the increase in Cd concentration decreases HOMO-LUMO gap is consistent with stability character shown by binding energy result.

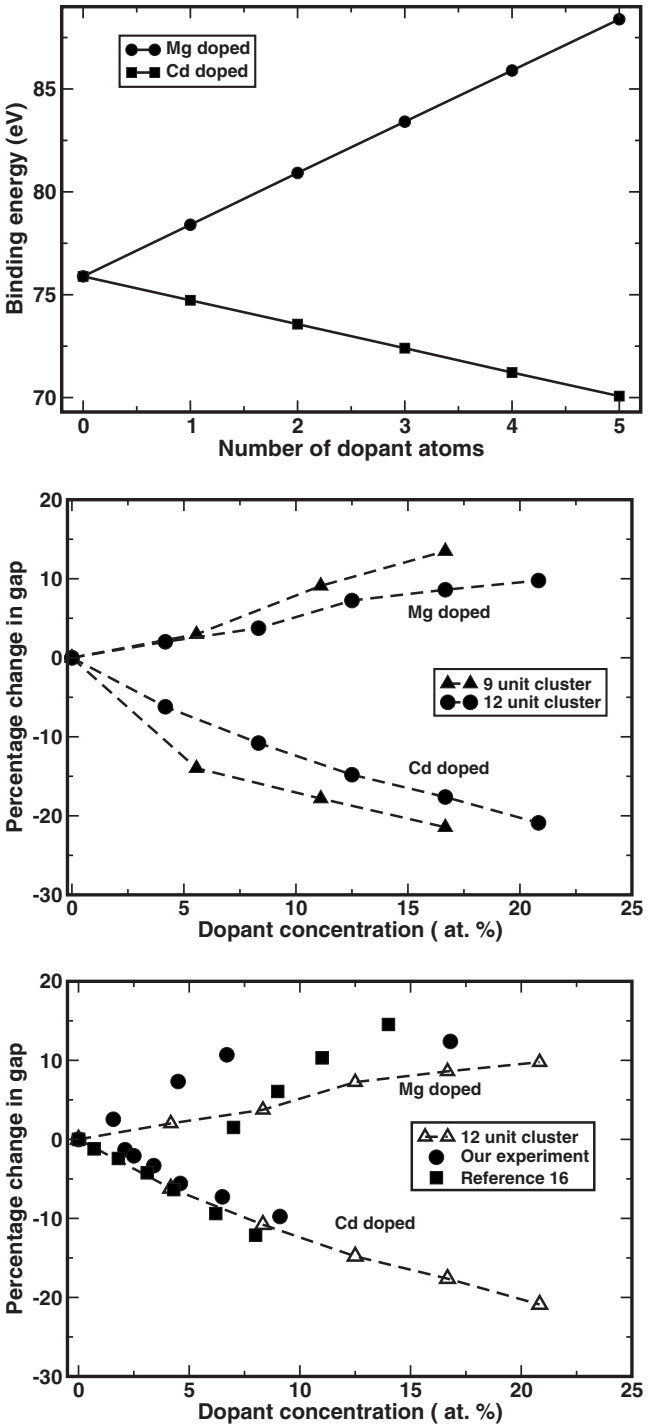

FIG. 9. (Left) Variation of the binding energy with Mg and Cd doping. (Middle) Variation in energy gaps with doping for $(ZnO)_n$ clusters for $n=9$ and 12. (Right) Variation of energy gaps with doping and comparison with experimental data on doped ZnO nanostructures. The dashed lines are shown for convenience of visualization.

Though it may be inappropriate to compare quantitatively the variation in the HOMO-LUMO gap of doped $(ZnO)_{12}$ clusters with that of band gap of rather larger nanostructures, it is interesting to note that the trend is qualitatively similar. We have also seen that as we increase the size of the cluster,

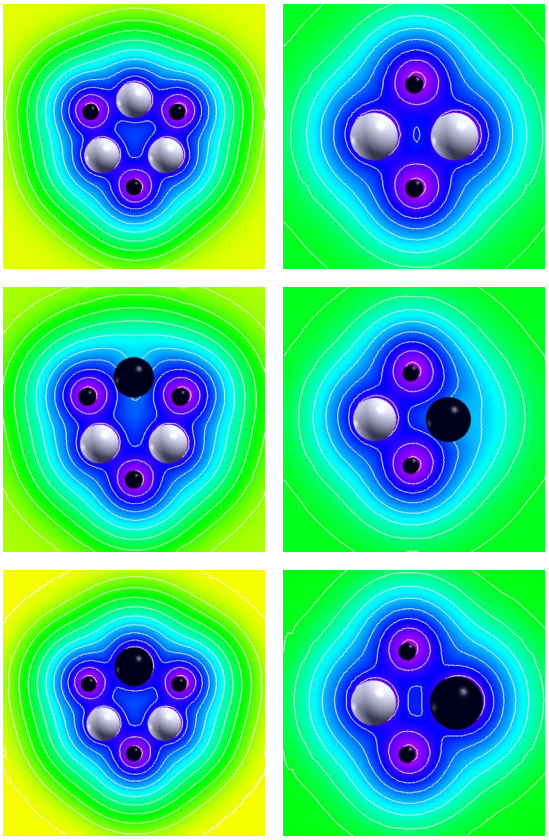

FIG. 10. (Color online) Charge densities of (left) pristine ZnO, (middle) Mg-doped ZnO, and (right) Cd-doped ZnO for (top) the $(ZnO)_3$ ring and (bottom) the $(ZnO)_2$ ring. Small black spheres represent O atoms, large white spheres represent Zn, and large black spheres are either Mg (middle column) or Cd (right column) atoms.

the change in the HOMO-LUMO gap seems to converge to a definite trend with doping concentration.

Can we try to analyze the effect of doping on the bonding charge density within the cluster and its consequent effect on the HOMO-LUMO gap? To answer this question, let us look at the cluster $(ZnO)_{12}$ and the two clusters $Mg_5Zn_7O_{12}$ and $Cd_5Zn_7O_{12}$. All the three clusters are constructed out of six-membered and four-membered rings. Let us look at the charge densities on planes through one of these rings. These are shown in Fig. 10. The figure shows the Zn^{2+}, Mg^{2+}, and Cd^{2+} ions sitting in the sea of valence electron cloud. As compared to the pristine ZnO cluster, wherever a Mg^{2+} ion sits, the charge density is pushed away from it toward the Zn^{2+} ions. The reverse is true wherever a Cd^{2+} sits. This ion appears to pull the electronic charge cloud toward it. This is much better seen from the charge density difference map between the doped and pristine clusters as shown in Fig. 11.

To understand why this should be so, we first note that the geometric structure of the atoms is not important, since the same phenomenon is apparent in both the four-membered and the six-membered rings. Figure 11 indicates that the electronegativity difference between Mg, Zn, and Cd and O decreases as we go from Mg to Cd. The $X-O$ (X=Mg, Zn, or Cd) bonds are partially ionic and partially covalent. If we relate the ionicity of the $X-O$ bond to the electronegativity difference between X and O, then MgO should be the most

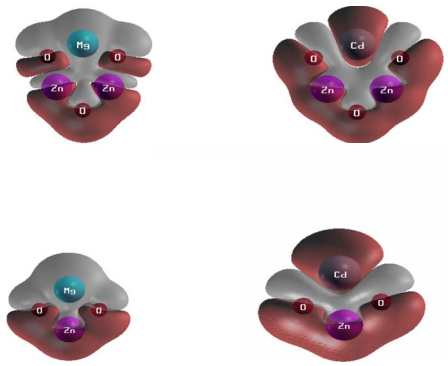

FIG. 11. (Color online) Difference in charge densities (left) between Mg-doped ZnO and pristine ZnO and (right) Cd-doped ZnO and pristine ZnO. The light gray shaded areas are of negative difference (charge depleted) and the black (red) areas of positive difference (charge accumulation).

ionic and CdO the least with ZnO in the middle. We can argue that this is so because the 3*s* energy level in Mg, 4*s* in Zn, and 5*s* in Cd decrease in this order. Consequently, the energy difference between these *s* levels and the O 2*p* level is smallest in CdO and increases for ZnO and largest in MgO. Thus, ionicity is lowest in CdO, larger in ZnO, and largest in CdO. This is now consistent with larger band gaps for $Mg_xZn_{1-x}O$ and smaller ones for $Cd_xZn_{1-x}O$ in the spirit of the ionicity theory of Phillips,[40] Nelson and Batra,[41] and Catlow and Stoneham[42] or the polarity theory of Harrison.[43,44]

This doping dependence of bond strength is also reflected in the fact that while the Zn-Zn distance in the pristine $(ZnO)_{12}$ is 2.60 Å on a six-membered ring, it reduces to 2.54 Å in the Mg-doped cluster. This is a sign of strengthened bonding between Zn atoms and in a simple tight-binding description leads to a larger overlap between tight-binding basis orbitals. For the Cd-doped cluster, this distance enlarges to 2.64 Å, indicating weakened bonding between Zn atoms and lower overlap between tight-binding basis orbitals. These local distortions should have their signature in Raman experiments and have a profound influence on the behavior of these clusters. In this simple bond by bond picture, there is a correlation between the gap and bonding energy. However, to make this quantitative is difficult and unclear to us at the present moment.

IV. CONCLUSION

We have carried out experimental investigation into the change of the "band gap" of nanosized structures of ZnO doped with Mg and Cd. Theoretical investigations on clusters of the ZnO doped with Mg and Cd show very similar trends in the change of the HOMO-LUMO gap. We have tried to understand the reason for this change from the changes in bonding strength on doping.

ACKNOWLEDGMENT

S.D. wishes to thank CSIR for financial support.

[1] P. J. Sebastian and M. Ocampo, Sol. Energy Mater. Sol. Cells **44**, 1 (1996).
[2] X. L. Guo, J. H. Tabata, and T. Kawai, Jpn. J. Appl. Phys., Part 2 **40**, L177 (2001).
[3] E. Corcoran, Sci. Am. **263** (5), 74 (1990).
[4] S. Krishnamoorthy, A. A. Iliadis, A. Inumpudi, S. Choopum, R. D. Vispute, and T. Venkatesan, Solid-State Electron. **46**, 1633 (2002).
[5] Z. Li, Y. Xiong, and Y. Xie, Inorg. Chem. **42**, 24 (2003).
[6] R. F. Mulligan, A. A. Iliadis, and P. Kofinas, J. Appl. Polym. Sci. **89**, 1058 (2003).
[7] M. H. Huang, S. Mao, H. Feick, H. Q. Yan, Y. Y. Wu, H. Kind, E. Weber, R. Russo, and P. D. Yang, Science **292**, 1897 (2001).
[8] H. Kind, H. Q. Yan, B. Messer, M. Law, and P. D. Yang, Adv. Mater. (Weinheim, Ger.) **14**, 158 (2001).
[9] R. Thangavel, M. Rajagopalan, and J. Kumar, Solid State Commun. **137**, 507 (2006).
[10] W. L. L. Lambrecht, S. Limpijumnong, and B. Segall, MRS Internet J. Nitride Semicond. Res. **4s1**, G6.8 (1999).
[11] A. C. Reber, S. N. Khanna, J. S. Hunjan, and M. R. Beltrán, Chem. Phys. Lett. **428**, 376 (2006).
[12] A. Ohotomo, M. Kawasaki, T. Koida, K. Masubuchi, H. Koinuma, Y. Sakurai, T. Yasuda, and Y. Segawa, Appl. Phys. Lett. **72**, 2466 (1998).
[13] A. K. Sharma, J. Narayan, J. F. Muth, C. W. Teng, C. Jin, A. Kevit, R. M. Kolbas, and O. W. Holland, Appl. Phys. Lett. **75**, 3327 (1999).
[14] F. Wang, Z. Ye, D. Ma, L. Zhu, and F. Zhuge, J. Cryst. Growth **283**, 373 (2005).
[15] T. Makino, Y. Segawa, M. Kawasaki, A. Ohotomo, R. Shiroki, K. Tamura, T. Yasuda, and H. Koinuma, Appl. Phys. Lett. **78**, 1237 (2001).
[16] L. M. Kukreja, S. Barik, and P. Mishra, J. Cryst. Growth **268**, 531 (2004).
[17] A. Kokalj, J. Mol. Graphics Modell. **17**, 176 (1999).
[18] P. Schroer, P. Kruger, and J. Pollmann, Phys. Rev. B **47**, 6971 (1993).
[19] P. Schroer, P. Kruger, and J. Pollmann, Phys. Rev. B **48**, 18264 (1993).
[20] P. Schroer, P. Kruger, and J. Pollmann, Phys. Rev. B **49**, 17092 (1994).
[21] D. Vogel, P. Kruger, and J. Pollmann, Phys. Rev. B **52**, R14316 (1995).
[22] D. Vogel, P. Kruger, and J. Pollmann, Phys. Rev. B **54**, 5495 (1996).
[23] J. M. Matxain, J. E. Fowler, and J. M. Ugalde, Phys. Rev. A **62**, 053201 (2000).
[24] J. M. Matxain, J. M. Mercero, J. E. Fowler, and J. M. Ugalde, J. Am. Chem. Soc. **125**, 9494 (2003).
[25] M. Ghosh and A. K. Raychaudhuri, J. Appl. Phys. **100**, 034315 (2006).
[26] R. Viswanatha, S. Sapra, B. Satpati, P. V. Satyam, B. N. Dev, and D. D. Sarma, J. Mater. Chem. **14**, 661 (2004).
[27] Y. S. Wang, P. John Thomas, and P. O'Brien, J. Phys. Chem. B **110**, 21412 (2006).
[28] M. Ghosh and A. K. Raychaudhuri, Nanotechnology **18**, 115618 (2007).
[29] G. K. Williamson and W. H. Hall, Acta Metall. **1**, 22 (1953).
[30] P. E. Blöchl, Phys. Rev. B **50**, 17953 (1994).
[31] G. Kressé and D. Joubert, Phys. Rev. B **59**, 1758 (1999).
[32] J. P. Perdew, J. A. Chevary, S. H. Vosko, K. A. Jackson, M. R. Pederson, D. J. Singh, and C. Fiolhais, Phys. Rev. B **46**, 6671 (1992).
[33] P. Pulay, Mol. Phys. **19**, 197 (1969).
[34] F. Calvo, Phys. Rev. B **67**, 161403(R) (2003).
[35] E. C. Behrman, R. K. Foehrweiser, J. R. Myers, B. R. French, and M. E. Zandler, Phys. Rev. A **49**, R1543 (1994).
[36] *CRC Handbook of Chemistry and Physics*, 58th ed. (CRC, Boca Raton, 1977).
[37] A. V. Bulgakov, I. Ozerov, and W. Marine, Thin Solid Films **453**, 557 (2004).
[38] H. Liu, S. Wang, G. Zhou, J. Wu, and W. Duan, J. Chem. Phys. **124**, 174705 (2006).
[39] H. S. Kang, S. H. Lim, J. W. Kim, H. W. Chang, G. H. Kim, J. Kim, S. Y. Lee, Y. Li, J. Lee, J. K. Lee, M. A. Nastasi, S. A. Crooker, and Q. X. Jia, J. Cryst. Growth **287**, 70 (2006).
[40] J. C. Phillips, Rev. Mod. Phys. **42**, 317 (1970).
[41] J. S. Nelson and I. P. Batra, Phys. Rev. B **39**, 3250 (1989).
[42] C. R. A. Catlow and A. M. Stoneham, J. Phys. C **16**, 4321 (1983).
[43] W. Harrison, Phys. Rev. B **10**, 767 (1974).
[44] W. Harrison, Phys. Rev. Lett. **34**, 1198 (1975).